Magnetic, electronic, structural, and thermal properties of the $Co_3O_2BO_3$ ludwigite in the paramagnetic state

C. W. Galdino,[1] D. C. Freitas,[2] C. P. C. Medrano,[2,3] R. Tartaglia,[1] D. Rigitano,[1] J. F. Oliveira,[3] A. A. Mendonça,[4] L. Ghivelder,[4] M. A. Continentino,[3] D. R. Sanchez,[2] and E. Granado[1]

[1] *"Gleb Wataghin" Institute of Physics, University of Campinas, Campinas, São Paulo 13083-859, Brazil*

[2] *Instituto de Física, Universidade Federal Fluminense, Campus da Praia Vermelha, Niterói, Rio de Janeiro 24210-346, Brazil*

[3] *Centro Brasileiro de Pesquisas Físicas, Rua Dr. Xavier Sigaud, 150 - Urca, Rio de Janeiro, Rio de Janeiro 22290-180, Brazil*

[4] *Instituto de Física, Universidade Federal do Rio de Janeiro, Caixa Postal 68528, Rio de Janeiro, Rio de Janeiro 21941-972, Brazil*

(Received 22 March 2019; revised manuscript received 30 August 2019; published 23 October 2019)

The mixed-valent homometallic ludwigite $(Co_2^{2+}Co^{3+})O_2BO_3$ is investigated above the ferrimagnetic ordering temperature $T_C = 43$ K through structural, thermal, magnetic, electric, and spectroscopic probes. X-ray absorption at the Co $L_{2,3}$ edges is consistent with the coexistence of Co^{2+} and Co^{3+} ions, as expected by the sample stoichiometry. Magnetic susceptibility shows a relatively large net paramagnetic moment per Co ion above room temperature, $p = 4.87$, indicating that the Co^{3+} ions are not in a pure low-spin configuration at high temperatures, also showing a non-Curie-Weiss behavior below 300 K. Electrical conductivity and differential scanning calorimetry measurements on single crystals indicate two phase transitions at ∼475 and ∼495 K. X-ray powder diffraction shows substantial lattice parameter anomalies below 500 K. These results indicate phase transitions associated with changes in the Co oxidation state in each of its four crystallographic sites. Such transitions are possibly dictated by a competition between (i) an ordered ground state with all Co^{3+} ions occupying the same crystallographic site and (ii) either partially or totally charge-disordered states that are favored at high temperatures due to their higher entropy.

DOI: 10.1103/PhysRevB.100.165138

I. INTRODUCTION

Homometallic ludwigites with the chemical formula $(M_2^{2+}M^{3+})O_2BO_3$ are mixed-valent complex oxides with potentially interesting physical phenomena. In fact, the most intensively investigated member of this family, $Fe_3O_2BO_3$, presents signatures of charge density wave (CDW) ordering, multiple magnetic transitions, and the coexistence of paramagnetism and magnetic ordering [1–6]. $Co_3O_2BO_3$, on the other hand, presents a single ferrimagnetic ordering temperature $T_C = 43$ K [2,7–9]. Also, a hybrid of reduced-multiwalled carbon nanotubes and $Co_3O_2BO_3$ have outstanding performance as an oxygen evolution reaction (OER) electrocatalyst, where the slow OER kinetics presents the main bottleneck regarding the storage of renewable energy and clean energy generation [10]. The novel catalyst containing $Co_3O_2BO_3$ has an overpotential lower than that for the state-of-the-art RuO_2 catalyst [11]. Such interesting properties of homometallic ludwigites may be related to a number of factors, such as the low-dimensional units in the complex ludwigite structure (see Fig. 1), the mixed valence of the transition-metal ions located at four distinct crystallographic sites, and the detailed spin state of each transition-metal ion in the structure.

Recently, neutron powder diffraction (NPD) was carried out for $Co_3O_2BO_3$. The Co ions on site 4 (see Fig. 1) was found to show a rather small ordered magnetic moment ($0.5\ \mu_B$), suggesting either a dominant low-spin (LS) configuration for Co^{3+} ions ($L = 0$, $S = 0$) at these sites below T_C or a large degree of magnetic disorder at this site even at the lowest temperatures [7]. The former hypothesis is consistent with density functional theory calculations that indicate a ground state with LS Co^{3+} ions at site 4 [15]. The ordered magnetic moments at the remaining transition-metal sites are consistent with Co^{2+} ions in a high-spin (HS) state [7]. On the other hand, a Curie-Weiss fit to magnetic susceptibility data between 150 and 250 K is suggestive of a significant contribution of Co^{3+} moments in the paramagnetic state [2], suggesting a crossover from a preferred Co^{3+} LS state below T_C to a preferred Co^{3+} HS state at higher temperatures.

This work extends the investigation of the Co^{3+} spin state and possible additional electronic phenomena in $Co_3O_2BO_3$ to a wider temperature interval, also employing a complementary set of experimental probes such as x-ray diffraction, magnetic susceptibility, differential scanning calorimetry (DSC), and DC resistivity measurements. Soft x-ray absorption measurements confirm the coexistence of Co^{2+} and Co^{3+} ions, as expected from the charge neutrality condition for the chemical formula. We find that the Curie-Weiss law is established only above ∼300 K, and the extracted paramagnetic moment is sufficiently large to exclude the scenario with Co^{3+} ions in a pure LS configuration above this temperature. Electrical conductivity and differential scanning calorimetry experiments taken on individual single crystals indicate two sharp consecutive phase transitions between 470 and 500 K. X-ray diffraction on a powdered sample shows lattice parameter anomalies below 500 K without any visible space-group change within our resolution and sensitivity. It is inferred

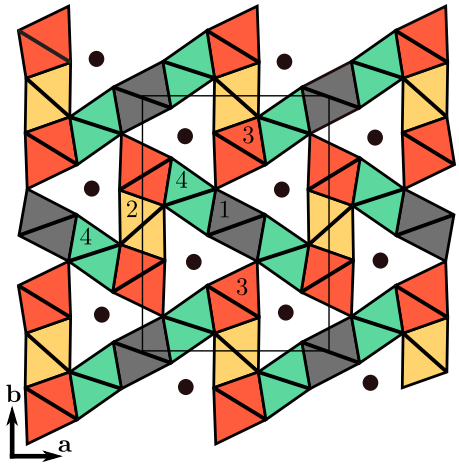

FIG. 1. Polyhedral representation of the ludwigite structure (space group *Pbam*) projected in the *ab* plane. The Co sites numbered from 1 to 4 are in the center of the corresponding oxygen octahedra, and the dots represent boron atoms. The unit cell is indicated by the rectangular thin black line. This structure is normally rationalized in terms of specific subunits such as the three-octahedra-wide ladders that extend along the **c** axis, one formed by edge-sharing octahedra 4-2-4 and the other formed by corner-sharing octahedra 3-1-3 (see Refs. [3,6,12–14]).

that two electronic phase transitions involving distinct spatial charge configurations of the Co ions take place in this material at high temperatures, with implications for the physics of ludwigites and other related families of materials.

II. EXPERIMENTAL DETAILS

Needle-shaped crystals of $Co_3O_2BO_3$ and $Co_5Sn(O_2BO_3)_2$ with typical dimensions of $\sim 50 \times 50 \times 700\ \mu m^3$ along the **a**, **b**, and **c** crystallographic directions, respectively, were synthesized through the procedure described in Refs. [2,16]. DC resistivity of $Co_3O_2BO_3$ was measured along the **c** direction by the four-probe method using a Keithley 2182A nanovoltmeter and a 6221 current source. The selected current $I = 30\ \mu A$ lies within a current interval where the resistivity shows Ohmic behavior. The employed heating/cooling rate was 2 K/min. The crystal was mounted on the copper cold finger of a closed-cycle He cryostat and was immersed in commercial thermal paste to minimize current leaks. Heat flow measurements were performed using a differential scanning calorimeter, model Q2000 from TA Instruments, following a heat/cool/heat procedure under a cooling/heating rate of 10 K/min between 250 and 550 K.

DC magnetic susceptibility measurements as a function of temperature were performed with $H = 10^4$ Oe. Due to the low mass of the individual crystals, a powder sample was prepared by grinding selected needle-shaped crystals to enhance the magnetic response, and the powder was tightly wrapped in a thin aluminum foil. Low-temperature measurements were performed with a superconducting quantum interference device magnetometer under warming after zero-field cooling, while high-temperature measurements were taken under warming on a vibrating sample magnetometer equipped with a furnace. For the latter, a spurious contribution arising from the sample support and Al foil was measured separately between 300 and 800 K and subtracted out of the raw signal.

For x-ray powder diffraction measurements, we employed a mix of thin powder and a bunch of small crystals taken from the same crucible where the larger crystals were grown. This polycrystalline sample was ground, sieved to $\sim 5\ \mu m$, deposited over a flat sample holder appropriate for Bragg-Brentano geometry, and mounted in a homemade furnace. The experiments were performed under ambient atmosphere at the XPD beamline of the Brazilian Synchrotron Light Laboratory (LNLS) with $\lambda = 1.7712$ Å [17]. The diffractograms were collected in the 10°–60° 2θ range between 300 and 700 K using a linear solid-state detector with 1280 pixels and 50-μm pixel size. Due to bad grain statistics and preferred orientation effects, a Rietveld structural refinement could not be performed, and the lattice parameters were obtained by the Le Bail method using the software FULLPROF [18]. A spurious Co_3O_4 phase was observed (see below), which is due to the fact that the needle-shaped crystals characteristic of the main ludwigite phase were not preselected in the specific sample preparation procedure for the diffraction experiment.

The x-ray absorption spectroscopy (XAS) spectra at the Co $L_{2,3}$ edges were taken at the PGM beamline of LNLS under the total electron yield mode, using a powdered sample of $Co_3O_2BO_3$ and a bunch of single crystals of $Co_5Sn(O_2BO_3)_2$. Spectra taken before and after scrapping the samples with a diamond file were identical. Due to the highly insulating character of $Co_3O_2BO_3$, spectra taken below room temperature were distorted due to surface charging effects [19], and therefore, only room-temperature data are used in this work.

III. RESULTS AND ANALYSIS

A. Magnetization and magnetic susceptibility

Figure 2 shows the magnetic susceptibility of $Co_3O_2BO_3$. The data below 250 K are consistent with previously reported results [2]. A Curie-Weiss behavior is observed above room temperature, and a linear fit $[\chi = C/(T - \Theta_{CW})]$ yields $\Theta_{CW} = -128$ K and $C = 8.91$ emu K mol(f.u.)$^{-1}$ Oe^{-1},

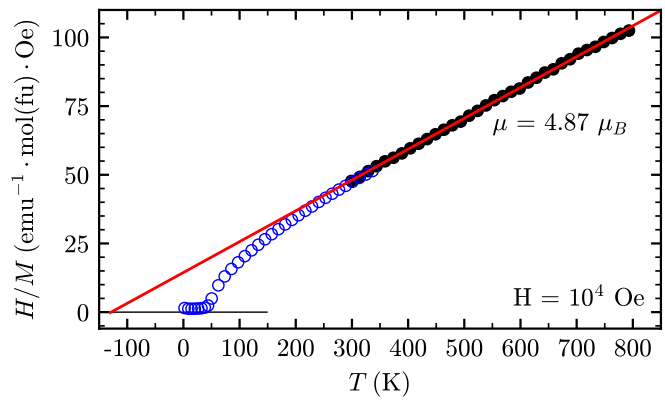

FIG. 2. Inverse of the magnetic susceptibility $\chi(T)^{-1}$, where the blue and black curves were taken using different instruments. The red solid line is the fit to the Curie-Weiss law for data above room temperature.

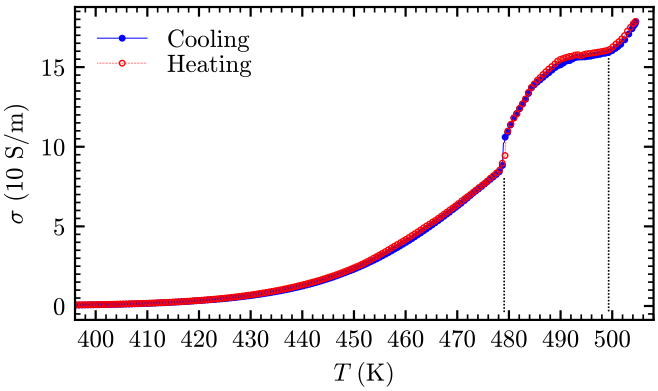

FIG. 3. Electrical conductivity $\sigma(T)$ of $Co_3O_2BO_3$, measured along the **c** direction on heating and cooling. The vertical dashed lines mark the identified phase transitions.

corresponding to a net paramagnetic moment per Co ion $p = 4.87$.

B. Electrical transport

Figure 3 shows the DC conductivity curves $\sigma(T)$ of $Co_3O_2BO_3$ between 396 and 505 K, taken along the **c** direction on both heating and cooling. The sample shows a nonmetallic behavior over the investigated temperature range, therefore retaining the same insulating behavior previously found below room temperature [20]. The conductivity shows a sharp rise at 479 K, indicative of a first-order phase transition. The temperature hysteresis for this transition is below the experimental error associated with the thermal inertia of our system (∼1 K). On further warming, a change in behavior of $\sigma(T)$ is noticed between ∼490 and 500 K, suggestive of another phase transition in this temperature interval.

C. Differential scanning calorimetry

Figure 4(a) shows heat flow measurements taken in a single-crystalline sample. The material presents phase transitions identified with two endothermic (exothermic) peaks under heating (cooling), at 472 and 493 K. Figure 4(b) shows the same data as Fig. 4(a) after subtracting an interpolated background to highlight the anomalies at the phase transitions. For comparison, similar data taken on the powder sample used in our temperature-dependent x-ray diffraction measurements (see below) are also shown in Fig. 4(b). The observed peaks in the DSC data are clearly related to the anomalies found in conductivity data at similar temperatures (see Fig. 3). The slight offset of ∼5 K between the transitions observed by DSC and resistivity correspond to only ∼1% of their absolute values and is attributed to a thermometry error. Notice that, in the background-subtracted data, between the two endothermic (exothermic) transformations upon heating (cooling) the crystal passes through an exothermic (endothermic) process. These results indicate that the compound presents a nontrivial three-way heat exchange process in an ∼20 K temperature interval, with an endo-exo-endothermic process in the heating curve and an exo-endo-exothermic process in the cooling curve.

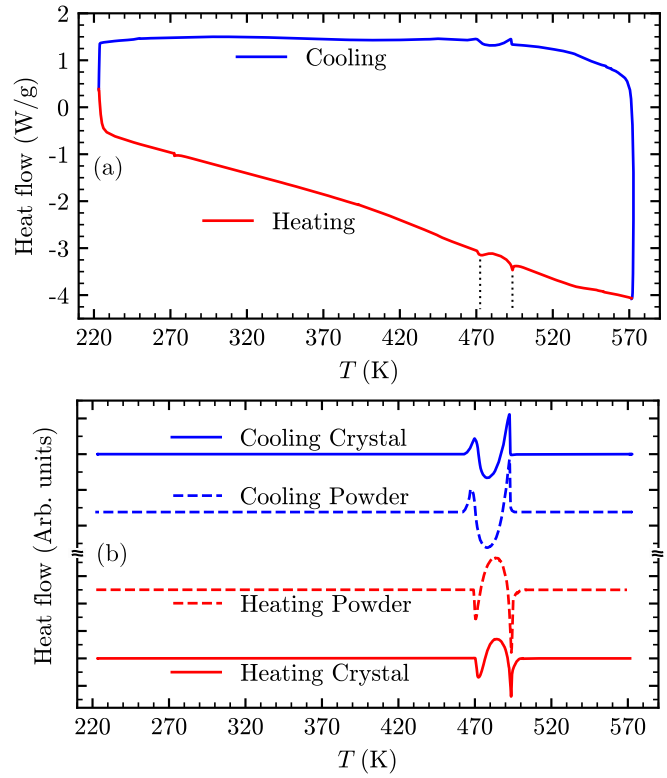

FIG. 4. (a) Heat flow as a function of temperature for a single crystal, taken on heating and cooling with a rate of 10 K/min. (b) Background-subtracted heat flow, highlighting the anomalies between 470 and 500 K, for a single crystal [using the raw data displayed in (a)] and the powder sample also employed in the x-ray diffraction experiment.

D. X-ray diffraction

Figures 5(a)–5(c) show the raw diffraction profiles at 300, 450, and 600 K, respectively. The observed peaks could be indexed under a main orthorhombic ludwigite phase with the *Pbam* space group and a Co_3O_4 impurity phase, indicating that no space group change is associated with the transitions revealed by electrical conductivity and heat flow measurements, at least within our resolution and sensitivity.

Figures 6(a)–6(d) show the orthorhombic lattice parameters a, b, and c and unit cell volume V as a function of temperature above 300 K. A contraction of a and expansion of c are observed below 500 K. The volumetric thermal expansion coefficient α_V rises significantly from $\alpha_V \equiv (1/V)(\partial V/\partial T)_P = 4.9 \times 10^{-5}$ K^{-1} below 400 K to $\alpha_V = 1.1 \times 10^{-4}$ K^{-1} above 500 K. No observable thermal hysteresis is identified.

Figure 7 shows in detail the c-lattice parameter in the 400–600 K interval. Slight anomalies can be seen at ∼475 and ∼495 K, corresponding to the phase transitions revealed by DSC and resistivity data.

E. X-ray absorption spectroscopy at the Co $L_{2,3}$ edges

Figure 8(a) displays the Co $L_{2,3}$ edges XAS spectra of $Co_3O_2BO_3$ and the Co^{2+} reference $Co_5Sn(O_2BO_3)_2$, together with reported spectra of the reference compounds Sr_2CoO_3Cl (Co^{3+} HS) and $EuCoO_3$ (Co^{3+} LS), both duplicated from

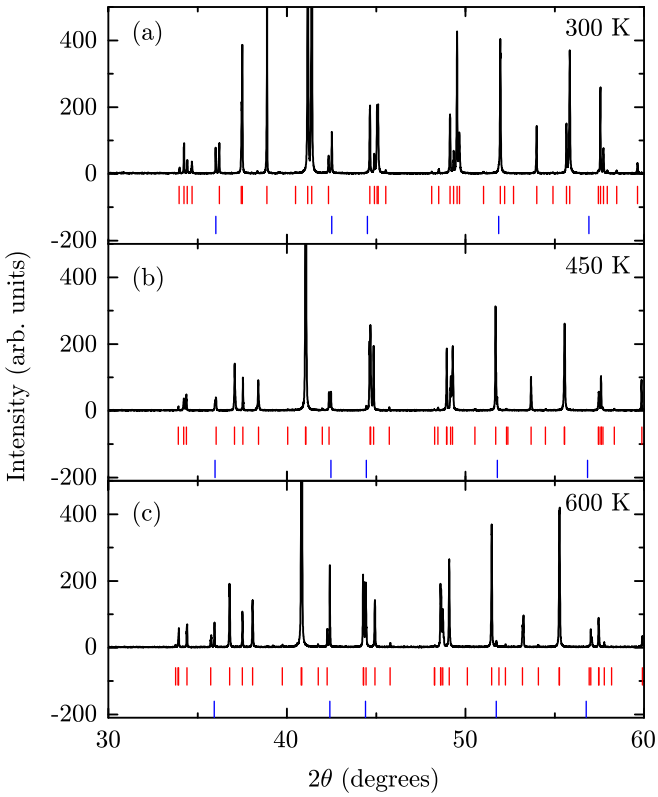

FIG. 5. Raw x-ray powder diffraction profiles taken at (a) $T =$ 300 K, (b) 450 K, and (c) 600 K with $\lambda = 1.7712$ Å. The vertical bars correspond to the Bragg positions of the main phase (space group *Pbam*, red) and of an impurity phase of Co_3O_4 (blue).

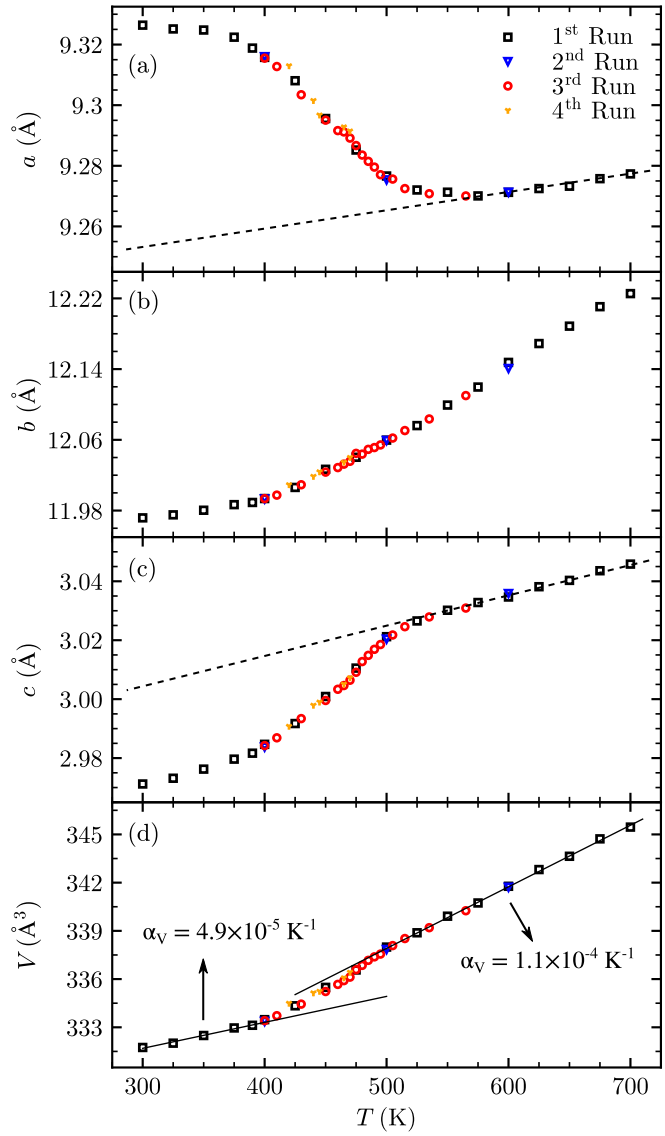

FIG. 6. (a)–(c) a, b, and c lattice parameters and (d) unit cell volume V as a function of temperature. Four runs of measurements were performed, two of them on warming (first and third runs) and two on cooling (second and fourth runs). In (d), the thermal expansion coefficient α_V is indicated for temperatures below 400 and above 500 K. Dashed lines in (a) and (c) correspond to the high-temperature linear behavior extrapolated down to 300 K.

Ref. [21], and CoO (Co^{2+}), duplicated from Ref. [22]. As expected, the spectrum of $Co_5Sn(O_2BO_3)_2$ resembles that of CoO since both are references for Co^{2+}. The spectroscopic signature of coexisting Co^{2+} and Co^{3+} ions in $Co_3O_2BO_3$ can be seen at both L_2 and L_3 edges. At the L_3 edge, the spectral weight of the $Co_3O_2BO_3$ XAS spectrum close to 780.3 eV [see dotted line in Fig. 8(a)] is stronger than for $Co_5Sn(O_2BO_3)_2$ or CoO. This is indicative of the Co^{3+} presence as the reference compounds Sr_2CoO_3Cl and $EuCoO_3$ show a sharp and intense peak at this energy. Moreover, such enhanced spectral weight at 780.3 eV in $Co_3O_2BO_3$ shifts the "center of gravity" of the spectrum to higher energies, which is in accordance with the general notion that higher-valence states shifts the spectra to higher energies [23,24].

Taking the Co $L_{2,3}$ absorption spectrum of $Co_5Sn(O_2BO_3)_2$ as a Co^{2+} reference in the ludwigite structure, we subtracted the spectrum of this sample from that of $Co_3O_2BO_3$ and therefore isolated the contribution from the Co^{3+} ions alone in the latter [see Fig. 8(b)], following the procedure described in Burnus *et al.* [22]. The spectra of both samples are normalized by the intensity of the lowest-energy peak at 777 eV, which is characteristic of octahedral Co^{2+}. Figure 8(b) shows that the difference spectrum resembles the Co^{3+} spectrum reported for both HS Sr_2CoO_3Cl and LS $EuCoO_3$, with particularly good agreement for the latter. However, considering the different crystal structures of these reference compounds with respect to the $Co_3O_2BO_3$ ludwigite, the uncertainties brought by the subtraction procedure described above, possible effects of nonrandom crystallite orientations, and also the similar HS and LS Co^{3+} reference XAS spectra, it is not possible to establish unambiguously the average spin state of the Co^{3+} ions in $Co_3O_2BO_3$ based on our XAS data alone.

IV. DISCUSSION

The effective moment per Co atom obtained from the Curie-Weiss fit above room temperature of the magnetic susceptibility data shown in Fig. 2 is $p = 4.87$. The expected spin-only moments are 3.87 and 4.90 for HS Co^{2+} and Co^{3+}, respectively. On the other hand, orbital magnetic moments

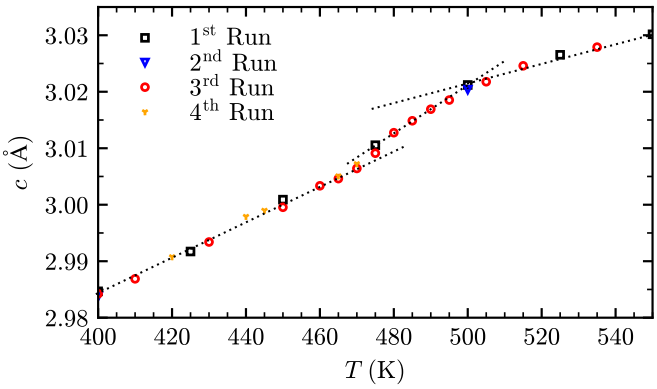

FIG. 7. Expanded view of the c lattice parameter in a selected temperature interval [see also Fig. 6(c)]. Dotted lines highlight the change in behavior in the interval between ~470 and ~500 K.

are potentially relevant. For instance, the observed moments for selected materials with Co^{2+} ions in octahedral environments are $p = 4.92$ in CoO, $p = 4.88$ in $Co(OH)_2$ [25], and $p = 5.18$ in $Co(CH_3SO_3)_2$ [26], which are significantly higher than the spin-only value. Anyway, the experimental paramagnetic moment observed for $Co_3O_2BO_3$ above room temperature is sufficiently large to exclude the possibility of all Co^{3+} ions being configured in a pure LS state with null magnetic moment.

The non-Curie-Weiss behavior observed below 300 K is suggestive of a gradual Co^{3+} spin state crossover towards a LS configuration below this temperature. Indeed, the paramagnetic moment extracted from the data between 150 and 250 K is only $p = 4.21$ per Co ion [2], significantly smaller than the high-temperature value $p = 4.88$, signaling a loss of magnetic moments on cooling. A dominant LS configuration for the Co^{3+} ions at low temperatures is supported by the small ordered Co magnetic moment of only 0.5 μ_B in site 4 at $T = 2$ K observed by neutron diffraction [7], and by density functional theory calculations [15]. Recent group theoretical analysis and semiempirical calculations of the superexchange interactions also support LS trivalent ions occupying site 4 at low temperatures, where the presence of nonmagnetic ions at this site removes frustration of exchange interactions, leading to long-range ferrimagnetic ordering in $Co_3O_2BO_3$ [27]. On the other hand, short-range spin correlations and crystal field effects may also lead to non-Curie-Weiss magnetic behavior at intermediate temperatures such as observed here; therefore, the possibility of a broad Co^{3+} spin state crossover at the paramagnetic phase below 300 K still needs to verified by other experimental techniques such as electron paramagnetic resonance. If confirmed, such a spin state crossover may be compared to other Co^{3+} oxides such as $LaCoO_3$, where the proportion of Co^{3+} ions in the HS state increases from 0% at the lowest temperatures to 40% at 650 K [28]. This phenomenon is the result of competing electronic configurations with similar energies for the Co^{3+} ions. The balance between these configurations may be changed upon heating, either directly by favoring a high-entropy state with coexisting LS and HS Co^{3+} ions or indirectly through the thermal expansion

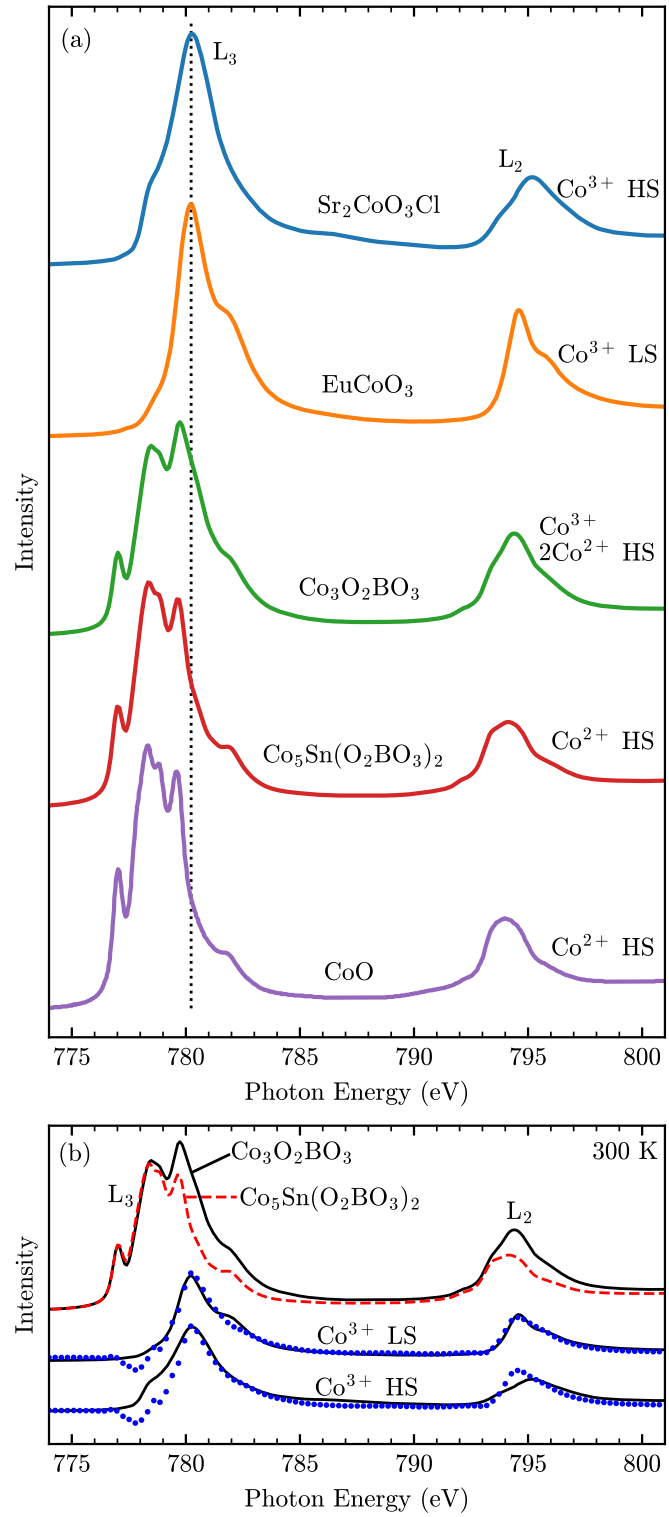

FIG. 8. (a) Co $L_{2,3}$ XAS spectra of Sr_2CoO_3Cl [21], $EuCoO_3$ [21], $Co_3O_2BO_3$, $Co_5Sn(O_2BO_3)_2$, and CoO [22] at room temperature. (b) Co $L_{2,3}$ XAS spectra of $Co_3O_2BO_3$ (upper solid line) scaled to the Co^{2+} reference compound $Co_5Sn(O_2BO_3)_2$ (red dashed curve). The corresponding difference spectrum (multiplied by 1.5 for better visualization) is given in blue solid symbols and compared to the Co^{3+} LS reference spectrum of $EuCoO_3$ (middle solid line) and the Co^{3+} HS reference spectrum Sr_2CoO_3Cl (lower solid line).

of the Co^{3+}-O bonds that tend to favor the HS state by reducing the crystal electric field splitting between the t_{2g} and e_g levels.

The only other known homometallic ludwigite, $Fe_3O_2BO_3$, presents a structural transition associated with a dimerization of the 424 ladders (see Fig. 1) that is evidenced by x-ray diffraction and magnetic susceptibility measurements [1]. Contrary to the Fe ludwigite, the $Co_3O_2BO_3$ system does not show dimer formation at the 424 ladder since such dimerization is inconsistent with the *Pbam* space group of $Co_3O_2BO_3$ found over the entire investigated temperature range. Note that recent *ab initio* density functional theory calculations indicate that LS Co^{3+} ions occupying site 4 may prevent the dimerization of the 424 ladder [15].

The high-temperature phase transitions observed by electrical conductivity (Fig. 3), DSC (Fig. 4), and x-ray diffraction (Figs. 6 and 7) remain to be discussed. Since the equilibrium state of a system minimizes the free energy $F \equiv U - TS$, where U is the energy and S is the entropy, high temperatures favor high-entropy states in general. In the present case, it is evident that a "charge-disordered" state, where the Co^{3+} ions are distributed over all four transition-metal sites, and/or partial charge-ordered states, where the charge mobility occurs over some specific sites, should be favored at high temperatures; therefore, electronic phase transitions involving distinct spatial distributions for the Co oxidation states in the lattice are the most plausible scenario to understand the observed transitions on warming. In fact, upon heating, the two endothermic transitions shown by the heat flow measurements [see Fig. 4(b)] are indicative of a two-stage melting process. These two transitions are also seen under cooling with an exothermic character, demonstrating that charge localization is recovered. It is interesting to note that between the two transitions the crystal seems to release (absorb) heat upon warming (cooling) [see Fig. 4(b)]. This heat release (absorption) might be related to a cross-linking between ladders.

With the data presently at hand, it is not possible to determine the specific spatial Co charge distributions in the phases above the transitions at ∼475 and 495 K. In fact, the complex crystal structure of the $Co_3O_2BO_3$ ludwigite with four distinct Co crystallographic sites (see Fig. 1) allows, in principle, for a number of charge-ordered, partially ordered, and disordered states. Nonetheless, a few conclusions may be drawn based on our electrical conductivity data (see Fig. 3). First of all, the state immediately above ∼475 K presents an increased conductivity along the c direction, pointing to an increased probability of electron or hole hopping between equivalent crystallographic sites at different rungs of the ladders (see Fig. 1). Further warming above ∼495 K seems to be detrimental to the conductivity along c (see Fig. 3). It is likely that the higher-temperature transition involves a delocalization of the quasiparticles inside the rungs in the ab plane that might deplete the hopping between different rungs along c. In short, it is plausible that the higher-temperature transition enhances the diversity of crystallographic sites possibly occupied by Co^{3+} ions without leading to an increment of the conductivity along the c direction. It is clear that additional electrical conductivity data along the a and b directions may provide valuable additional information. Unfortunately, such measurements are challenging due to the needlelike shapes of the $Co_3O_2BO_3$ crystals and are beyond the scope of the present work.

According to our x-ray power diffraction data, the electronic transitions discussed above do not appear to change the space group symmetry of $Co_3O_2BO_3$. On the other hand, an interesting behavior of the a and c lattice parameters is observed, most notably in the temperature range between 400 and 500 K (Fig. 6). The broad temperature range where the unconventional lattice behavior occurs is not attributable to a hypothetical lower quality of the powder sample with respect to single crystals since heat flow measurements on the same powder sample resulted in sharp anomalies that are very similar to single-crystal data [see Fig. 4(b)]. Also, the deviation of the a and c lattice parameters from the linear behavior observed at high temperatures [dashed lines in Figs. 6(a) and 6(c)] occurs most notably within the charge-ordered regime, i.e., for $T \lesssim 500$ K. Therefore, it is plausible that the a and c lattice parameter anomalies below ∼500 K are manifestations of temperature-dependent "charge order parameters" that may couple to the lattice and, in close analogy to, e.g., magnetic order parameters, vary appreciably over a wide temperature interval below the corresponding critical temperatures. It is interesting to mention that the transitions at ∼475 and ∼495 K seen by DSC and resistivity data are clearly manifested in the x-ray diffraction data through small but perceptible anomalies in the c lattice parameter (see Fig. 7).

In the Mn-substituted ludwigite $Co^{2+}_{1.37}Mn^{2+}_{0.63}Co^{3+}_{0.35}Mn^{3+}_{0.65}(O_2BO_3)^{7-}$, the Curie-Weiss fit of the magnetic susceptibility up to 200 K led to an effective magnetic moment consistent with trivalent HS Co ions [29]. Interestingly, the presence of Mn ions increases lattice parameters b and c, as well as the unit cell volume V, and reduces lattice parameter a compared to the parent compound $Co_3O_2BO_3$ at room temperature. Thus, a substitution of an ion with a larger ionic radius such as Mn^{3+} in site 4 of the Co ludwigite seems to lead to modifications in the lattice parameters and unit cell volume that have the same sign as the temperature-driven anomalies observed here for the pure material on heating above 400 K. The same trend is also observed in other mixed Co ludwigites such as $Co_{2.4}Ga_{0.6}O_2BO_3$ [30] and $Co_{2.25}Fe_{0.75}O_2BO_3$ [31]. Thus, the lattice parameter anomalies of $Co_3O_2BO_3$ on heating above ∼400 K are consistent with an increase of the average size of the Co ions at site 4, possibly occurring as a consequence of the melting of the charge-ordered state.

Charge melting transitions are observed in many other transition-metal oxides. For instance, the iron parent compound of the related warwickite structure, Fe_2OBO_3, is known to present two anomalies in the electrical conductivity at ∼300 and 340 K. Whereas the first discontinuity is associated with a monoclinic-orthorhombic transition in conjunction with a charge-ordering Verwey-like transition [32,33], the higher-temperature discontinuity is rationalized purely in terms of electron mobility between Fe ions with different valences without an accompanying structural transition [33,34]. Another compound that presents a lattice distortion accompanied by a sharp decrease in its conductivity (related to Fe^{2+}/Fe^{3+} charge ordering) is the naturally occurring iron oxide magnetite (Fe_3O_4) [35]. Two charge ordering mechanisms may be

relevant in transition-metal oxides: (1) electrostatic repulsion mechanisms, where ions are kept in place by strong electrostatic repulsion, and (2) strains arising from electron-lattice interactions, where distortions (such as Jahn-Teller) segregate ions between the crystallographic sites minimizing elastic strain. For the iron warwickite and Fe_3O_4, for example, the mechanism inducing charge order is believed to be a combination of the two mechanisms [33,34,36,37]. In $Co_3O_2BO_3$, the detailed charge-ordering mechanism is still unclear, although the correspondence between the charge-ordering transitions and the lattice parameter anomalies suggests that the strain mechanism is relevant. In any case, the existence of a two-stage charge-melting transition on warming evidenced by our measurements seems to be a particularity of the complex ludwigite structure with four distinct transition-metal sites.

V. CONCLUSIONS

In summary, we investigated magnetic, electronic, structural, and thermal properties of $Co_3O_2BO_3$ using a handful of experimental techniques. We confirm the coexistence of Co^{2+} and Co^{3+} ions in $Co_3O_2BO_3$ and the absence of trivalent ions in the Sn-doped $Co_5Sn(O_2BO_3)_2$ through XAS at the Co $L_{2,3}$ edges, as expected from the charge neutrality condition of the chemical formula. The non-Curie-Weiss behavior of the magnetic susceptibility above $T_C = 43$ K up to at least ~300 K [see Fig. 2(a)] is suggestive of a gradual Co^{3+} spin-state crossover, similar to $LaCoO_3$. Two consecutive sharp electronic transitions were observed at ~475 and 495 K in $Co_3O_2BO_3$ by heat flow and electrical conductivity measurements. Lattice parameter anomalies were observed below ~500 K. The observed transitions at high temperature are interpreted in terms of a two-step delocalization of the Co^{3+} hole that deserves further investigation.

ACKNOWLEDGMENTS

We thank F. Béron, R. R. Urbano, H. Tolentino, J. Souza, and P. Menegasso for helpful discussions and technical support. This work was supported by CNPq Grants No. 134752/2016-3, No. 308607/2018-0, and No. 142555/2018-5, FAPESP Grant No. 2018/20142-8, and CAPES, Brazil.

[1] M. Mir, R. B. Guimaraes, J. C. Fernandes, M. A. Continentino, A. C. Doriguetto, Y. P. Mascarenhas, J. Ellena, E. E. Castellano, R. S. Freitas, and L. Ghivelder, Structural Transition and Pair Formation in $Fe_3O_2BO_3$, Phys. Rev. Lett. **87**, 147201 (2001).

[2] D. C. Freitas, M. A. Continentino, R. B. Guimarães, J. C. Fernandes, J. Ellena, and L. Ghivelder, Structure and magnetism of homometallic ludwigites: Co_2OBO_3 versus Fe_2OBO_3, Phys. Rev. B **77**, 184422 (2008).

[3] R. B. Guimarães, M. Mir, J. C. Fernandes, M. A. Continentino, H. A. Borges, G. Cernicchiaro, M. B. Fontes, D. R. S. Candela, and E. Baggio-Saitovich, Cation-mediated interaction and weak ferromagnetism in $Co_2FeO_2BO_3$, Phys. Rev. B **60**, 6617 (1999).

[4] J. Larrea J., D. R. Sánchez, F. J. Litterst, E. M. Baggio-Saitovitch, J. C. Fernandes, R. B. Guimarães, and M. A. Continentino, Magnetism and charge ordering in $Fe_3O_2BO_3$ studied by ^{57}Fe Mössbauer spectroscopy, Phys. Rev. B **70**, 174452 (2004).

[5] P. Bordet and E. Suard, Magnetic structure and charge ordering in Fe_3BO_5: A single-crystal x-ray and neutron powder diffraction study, Phys. Rev. B **79**, 144408 (2009).

[6] M.-H. Whangbo, H.-J. Koo, J. Dumas, and M. Continentino, Theoretical investigation of the spin exchange interactions and magnetic properties of the homometallic ludwigite $Fe_3O_2BO_3$, Inorg. Chem. **41**, 2193 (2002).

[7] D. C. Freitas, C. P. C. Medrano, D. R. Sanchez, M. N. Regueiro, J. A. Rodríguez-Velamazán, and M. A. Continentino, Magnetism and charge order in the ladder compound $Co_3O_2BO_3$, Phys. Rev. B **94**, 174409 (2016).

[8] N. Ivanova, N. Kazak, Y. V. Knyazev, D. Velikanov, L. Bezmaternykh, S. Ovchinnikov, A. Vasiliev, M. Platunov, J. Bartolomé, and G. Patrin, Crystal structure and magnetic anisotropy of ludwigite $Co_2FeO_2BO_3$, J. Exp. Theor. Phys. **113**, 1015 (2011).

[9] J. Bartolomé, A. Arauzo, N. V. Kazak, N. B. Ivanova, S. G. Ovchinnikov, Y. V. Knyazev, and I. S. Lyubutin, Uniaxial magnetic anisotropy in $Co_{2.25}Fe_{0.75}O_2BO_3$ compared to $Co_3O_2BO_3$ and Fe_3O_2BO ludwigites, Phys. Rev. B **83**, 144426 (2011).

[10] E. Fabbri, A. Habereder, K. Waltar, R. Kötz, and T. J. Schmidt, Developments and perspectives of oxide-based catalysts for the oxygen evolution reaction, Catal. Sci. Technol. **4**, 3800 (2014).

[11] S. Kundu, B. Malik, D. K. Pattanayak, and V. K. Pillai, Mixed valent, distorted cobalt ludwigite (Co_3BO_5/$Co_3O_2BO_3$) and its composite with reduced multiwalled carbon nanotubes (R-MWCNT) in enhancing the domain edge-sharing oxygen as superior water oxidation electrocatalysts, ChemElectroChem **5**, 1670 (2018).

[12] Y. Takéuchi, T. Watanabé, and T. Ito, The crystal structures of warwickite, ludwigite and pinakiolite, Acta Cryst. **3**, 98 (1950).

[13] M. Continentino, J. Fernandes, H. Borges, A. Sulpice, J.-L. Tholence, J. Siqueira, J. da Cunha, C. dos Santos *et al.*, Magnetic interactions in the monoclinic ludwigite CuFeOBO, Eur. Phys. J. B **9**, 613 (1999).

[14] J. C. Fernandes, R. B. Guimarães, M. A. Continentino, H. A. Borges, A. Sulpice, J. L. Tholence, J. L. Siqueira, L. I. Zawislak, J. B. M. daCunha, and C. A. dosSantos, Magnetic interactions in the ludwigite $Ni_2FeO_2BO_3$, Phys. Rev. B **58**, 287 (1998).

[15] M. O. M. Matos, J. Terra, and D. Ellis, Low lying magnetic states of the mixed valence cobalt ludwigite, Phys. Status Solidi B 1900298 (2019).

[16] C. P. C. Medrano, D. C. Freitas, D. R. Sanchez, C. B. Pinheiro, G. G. Eslava, L. Ghivelder, and M. A. Continentino, Nonmagnetic ions enhance magnetic order in the ludwigite $Co_5Sn(O_2BO_3)_2$, Phys. Rev. B **91**, 054402 (2015).

[17] F. F. Ferreira, E. Granado, W. Carvalho, Jr, S. W. Kycia, D. Bruno, and R. Droppa, Jr, X-ray powder diffraction beamline at D10B of LNLS: application to the Ba_2FeReO_6 double perovskite, J. Synchrotron Rad. **13**, 46 (2006).

[18] J. Rodríguez-Carvajal, Recent advances in magnetic structure determination by neutron powder diffraction, Phys. B (Amsterdam, Neth.) **192**, 55 (1993).

[19] D. Vlachos, A. J. Craven, and D. W. McComb, Specimen charging in X-ray absorption spectroscopy: Correction of total electron yield data from stabilized zirconia in the energy range 250-915 eV, J. Synchrotron Radiat. **12**, 224 (2005).

[20] N. Ivanova, A. Vasil'ev, D. Velikanov, N. Kazak, S. Ovchinnikov, G. Petrakovskiĭ, and V. Rudenko, Magnetic and electrical properties of cobalt oxyborate Co_3BO_5, Phys. Solid State **49**, 651 (2007).

[21] Z. Hu, H. Wu, M. W. Haverkort, H. H. Hsieh, H. J. Lin, T. Lorenz, J. Baier, A. Reichl, I. Bonn, C. Felser, A. Tanaka, C. T. Chen, and L. H. Tjeng, Different Look at the Spin State of Co^{3+} Ions in a CoO_5 Pyramidal Coordination, Phys. Rev. Lett. **92**, 207402 (2004).

[22] T. Burnus, Z. Hu, H. H. Hsieh, V. L. J. Joly, P. A. Joy, M. W. Haverkort, H. Wu, A. Tanaka, H. J. Lin, C. T. Chen, and L. H. Tjeng, Local electronic structure and magnetic properties of $LaMn_{0.5}Co_{0.5}O_3$ studied by x-ray absorption and magnetic circular dichroism spectroscopy, Phys. Rev. B **77**, 125124 (2008).

[23] C. Chen and F. Sette, High resolution soft X-ray spectroscopies with the Dragon beamline, Phys. Scr. **T31**, 119 (1990).

[24] C. Mitra, Z. Hu, P. Raychaudhuri, S. Wirth, S. I. Csiszar, H. H. Hsieh, H. J. Lin, C. T. Chen, and L. H. Tjeng, Direct observation of electron doping in $La_{0.7}Ce_{0.3}MnO_3$ using x-ray absorption spectroscopy, Phys. Rev. B **67**, 092404 (2003).

[25] J. Richardson and L. Vernon, The magnetic properties of the cobalt oxide–alumina system, J. Phys. Chem. **62**, 1153 (1958).

[26] A. L. Arduini, M. Garnett, R. C. Thompson, and T. C. Wong, Magnetic and spectral studies on cobalt (ii) and copper (ii) salts of methylsulfuric, trifluoromethylsulfuric, and paratolylsulfuric acids, Can. J. Chem. **53**, 3812 (1975).

[27] Y. V. Knyazev, N. Kazak, I. Nazarenko, S. Sofronova, N. Rostovtsev, J. Bartolomé, A. Arauzo, and S. Ovchinnikov, Effect of magnetic frustrations on magnetism of the Fe_3BO_5 and Co_3BO_5 ludwigites, J. Magn. Magn. Mater. **474**, 493 (2019).

[28] M. W. Haverkort, Z. Hu, J. C. Cezar, T. Burnus, H. Hartmann, M. Reuther, C. Zobel, T. Lorenz, A. Tanaka, N. B. Brookes *et al.*, Spin State Transition in $LaCoO_3$ Studied Using Soft x-Ray Absorption Spectroscopy and Magnetic Circular Dichroism, Phys. Rev. Lett. **97**, 176405 (2006).

[29] Y. V. Knyazev, N. Ivanova, N. Kazak, M. Platunov, L. Bezmaternykh, D. A. Velikanov, A. D. Vasiliev, S. Ovchinnikov, and G. Yu. Yurkin, Crystal structure and magnetic properties of Mn substituted ludwigite $Co_3O_2BO_3$, J. Magn. Magn. Mater. **324**, 923 (2012).

[30] N. Ivanova, M. Platunov, Y. V. Knyazev, N. Kazak, L. Bezmaternykh, A. Vasiliev, S. Ovchinnikov, and V. Nizhankovskii, Effect of the diamagnetic dilution on the magnetic ordering and electrical conductivity in the $Co_3O_2BO_3$:Ga ludwigite, Phys. Solid State **54**, 2212 (2012).

[31] N. Kazak, N. Ivanova, O. Bayukov, S. Ovchinnikov, A. Vasiliev, V. Rudenko, J. Bartolomé, A. Arauzo, and Y. V. Knyazev, The superexchange interactions in mixed Co–Fe ludwigite, J. Magn. Magn. Mater. **323**, 521 (2011).

[32] J. Attfield, A. Bell, L. Rodriguez-Martinez, J. Greneche, R. Cernik, J. Clarke, and D. Perkins, Electrostatically driven charge-ordering in Fe_2OBO_3, Nature (London) **396**, 655 (1998).

[33] M. Angst, P. Khalifah, R. P. Hermann, H. J. Xiang, M.-H. Whangbo, V. Varadarajan, J. W. Brill, B. C. Sales, and D. Mandrus, Charge Order Superstructure with Integer Iron Valence in Fe_2OBO_3, Phys. Rev. Lett. **99**, 086403 (2007).

[34] M. Angst, R. P. Hermann, W. Schweika, J.-W. Kim, P. Khalifah, H. J. Xiang, M.-H. Whangbo, D.-H. Kim, B. C. Sales, and D. Mandrus, Incommensurate Charge Order Phase in Fe_2OBO_3 due to Geometrical Frustration, Phys. Rev. Lett. **99**, 256402 (2007).

[35] E. Verwey, Electronic conduction of magnetite (Fe_3O_4) and its transition point at low temperatures, Nature (London) **144**, 327 (1939).

[36] I. Leonov, A. N. Yaresko, V. N. Antonov, M. A. Korotin, and V. I. Anisimov, Charge and Orbital Order in Fe_3O_4, Phys. Rev. Lett. **93**, 146404 (2004).

[37] H.-T. Jeng, G. Y. Guo, and D. J. Huang, Charge-orbital Ordering and Verwey Transition in Magnetite, Phys. Rev. Lett. **93**, 156403 (2004).